PHYSICS OF FLUIDS **26**, 122105 (2014)

The effects of variable fluid properties on thin film stability

S. J. D. D'Alessio,[1,a)] C. J. M. P. Seth,[1,b)] and J. P. Pascal[2,c)]
[1]*Department of Applied Mathematics, University of Waterloo, Waterloo, Ontario N2L 3G1, Canada*
[2]*Department of Mathematics, Ryerson University, Toronto, Ontario M5B 2K3, Canada*

(Received 17 May 2014; accepted 24 November 2014; published online 18 December 2014)

A theoretical investigation has been conducted to study the impact of variable fluid properties on the stability of gravity-driven flow of a thin film down a heated incline. The incline is maintained at a uniform temperature which exceeds the temperature of the ambient gas above the fluid and is thus responsible for heating the thin fluid layer. The variable fluid properties are allowed to vary linearly with temperature. It is assumed that long-wave perturbations are most unstable. Based on this, a stability analysis was carried out whereby the governing linearized perturbation equations were expanded in powers of the wavenumber which is a small parameter. New interesting results illustrating how the critical Reynolds number and perturbation phase speed depend on the various dimensionless parameters have been obtained. © *2014 AIP Publishing LLC*. [http://dx.doi.org/10.1063/1.4904095]

I. INTRODUCTION

It is well known that the gravity-driven flow of a thin fluid layer down an inclined surface is prone to interfacial instabilities which become manifest as waves propagating along the free surface. This was first observed experimentally by Kapitza and Kapitza.[1] The first theoretical investigations to predict the onset of instability for isothermal flows were conducted by Benjamin[2] and Yih.[3] In these studies, the stability of the uniform flow was determined by linearizing the governing perturbation equations. To make analytical progress, an asymptotic expansion in the wavenumber was carried out since long-wave perturbations are most unstable.

For non-isothermal flows, it is well known that variations in surface tension give rise to thermocapillary effects which act to destabilize the flow; this phenomenon is referred to as the Marangoni effect. The Marangoni number is a dimensionless parameter which measures variations in surface tension. Previous studies[4,5] focusing on long-wave perturbations have successfully established the relationship between the critical Reynolds number and the Marangoni number. The general consensus is that for sufficiently thin fluid layers, the influence of density and viscosity variations is negligible in comparison with those in surface tension. Indeed, Ogden *et al.*[6] have shown that if the variations in density and viscosity are small, and in particular of the same order of magnitude as the wavenumber of unstable perturbations, then the critical Reynolds number for the onset of instability is unaffected by these variations. However, for larger variations, one can no longer make the simplifying assumption of ignoring variations in density and viscosity. Larger variations have been considered by Goussis and Kelly[7] and later by Hwang and Weng.[8] However, these investigations only consider the temperature variation in viscosity, and furthermore assume a constant temperature at the free surface which eliminates the Marangoni effect. Kabova and Kuznetsov,[9] on the other hand, include both variable viscosity and the Marangoni effect, but they only consider the steady-state problem.

a)email: sdalessio@uwaterloo.ca
b)email: cjmpseth@uwaterloo.ca
c)email: jpascal@ryerson.ca

Recently, Pascal *et al.*[10] examined the stability of the flow when the fluid properties were allowed to vary linearly with temperature. Asymptotic expansions for the critical Reynolds number predicting the onset of instability in the limit of small parameter values were constructed. The present research represents an extension of that reported in Ref. 10 where we again limit our attention to a planar substrate. As we will see the problem is sufficiently complicated, and extending it to a non-planar surface would make the problem intractable. In contrast to Ref. 10, exact expressions for the critical Reynolds number have been derived having no restrictions on the values of the parameters.

The paper is organized as follows. In Sec. II, we present the mathematical formulation, governing equations, and boundary conditions. Then in Sec. III, we perform a linear stability analysis. New interesting results are presented and discussed in Sec. IV. Finally, the research is summarized in the concluding Sec. V.

II. GOVERNING EQUATIONS

We consider the laminar two-dimensional flow of a thin viscous fluid layer down an impermeable planar surface which is inclined at an angle β with the horizontal. The adopted (x, z) Cartesian coordinate system is oriented so that the x-axis points down the incline and the z-axis points into the fluid layer. The velocity components in the x, z directions are denoted by u, w, respectively, while the position of the free surface is given by $z = h(x,t)$. The incline is maintained at a constant temperature, T_b, which exceeds the temperature of the ambient gas, T_a, above the fluid layer. The temperature difference $\Delta T = T_b - T_a$ is responsible for heating the thin fluid layer.

In the absence of viscous dissipation, the governing equations for a Newtonian fluid possessing variable fluid properties are given by[11]

$$\frac{D\rho}{Dt} + \rho\left(\frac{\partial u}{\partial x} + \frac{\partial w}{\partial z}\right) = 0\,, \tag{1}$$

$$\rho\frac{Du}{Dt} = -\frac{\partial p}{\partial x} + g\rho\sin\beta + \frac{\partial}{\partial x}\left[2\mu\frac{\partial u}{\partial x} - \frac{2}{3}\mu\left(\frac{\partial u}{\partial x} + \frac{\partial w}{\partial z}\right)\right] + \frac{\partial}{\partial z}\left[\mu\left(\frac{\partial u}{\partial z} + \frac{\partial w}{\partial x}\right)\right]\,, \tag{2}$$

$$\rho\frac{Dw}{Dt} = -\frac{\partial p}{\partial z} - g\rho\cos\beta + \frac{\partial}{\partial z}\left[2\mu\frac{\partial w}{\partial z} - \frac{2}{3}\mu\left(\frac{\partial u}{\partial x} + \frac{\partial w}{\partial z}\right)\right] + \frac{\partial}{\partial x}\left[\mu\left(\frac{\partial u}{\partial z} + \frac{\partial w}{\partial x}\right)\right]\,, \tag{3}$$

$$\rho\frac{De}{Dt} = \frac{\partial}{\partial x}\left(K\frac{\partial T}{\partial x}\right) + \frac{\partial}{\partial z}\left(K\frac{\partial T}{\partial z}\right) - p\left(\frac{\partial u}{\partial x} + \frac{\partial w}{\partial z}\right)\,, \tag{4}$$

where $\frac{D}{Dt}$ denotes the two-dimensional material derivative, p is the pressure, T is the temperature, g is the acceleration due to gravity, μ is the dynamic viscosity, ρ is the mass density, K is the thermal conductivity, and e is the internal energy.

A standard approach is to allow the fluid properties to vary linearly with temperature as follows:

$$\begin{aligned}
\rho &= \rho_0 - \hat{\alpha}(T - T_a)\,,\\
\mu &= \mu_0 - \hat{\lambda}(T - T_a)\,,\\
K &= K_0 + \hat{\Lambda}(T - T_a)\,,\\
\sigma &= \sigma_0 - \gamma(T - T_a)\,,
\end{aligned}$$

where σ is the surface tension, and $\hat{\alpha}$, γ, $\hat{\lambda}$, $\hat{\Lambda}$ are positive parameters measuring the rate of change with respect to temperature. Here, ρ_0, μ_0, K_0, and σ_0 represent values of the density, viscosity, thermal conductivity, and surface tension, respectively, at the reference temperature $T = T_a$. The study by Hwang and Weng[8] considered viscosity variations governed by an Arrhenius-type relation given in dimensionless form by

$$\frac{\mu}{\mu_0} = \exp\left[-Ar\frac{(T - T_a)}{T_a}\right]\,,$$

where Ar is the Arrhenius number. Although this may provide a more accurate description of viscosity variations with temperature, the problem becomes far more complicated. As we will shortly see, even the linear relation makes the problem quite difficult.

Using the first law of thermodynamics and applying standard thermodynamic relationships, the energy equation (4) can be rewritten as[12]

$$\rho c_p \frac{DT}{Dt} - \frac{\hat{\alpha} T}{\rho_0} \frac{Dp}{Dt} = \frac{\partial}{\partial x}\left(K \frac{\partial T}{\partial x}\right) + \frac{\partial}{\partial z}\left(K \frac{\partial T}{\partial z}\right) , \tag{5}$$

where c_p is the specific heat at constant pressure. Unlike ρ, μ, K, and σ which are allowed to vary linearly with temperature, c_p is taken to remain constant in this study. Outlined in Ref. 12 is a careful scaling analysis which specifies when the Boussinesq approximation applies and also when the term $\frac{\hat{\alpha} T}{\rho_0} \frac{Dp}{Dt}$ in Eq. (5) can be ignored; the condition

$$\varepsilon = \frac{\hat{\alpha} g L T_0}{\rho_0 c_p \Delta T} \ll 1$$

guarantees both of these. Here, L is a length scale, T_0 denotes T_a measured in Kelvin, and ΔT is a temperature difference scale. For flows of interest in this study, it turns out that ε is indeed small. For example, for a thin layer of water having $L = 5$ mm and $\Delta T = 5$ K with T_a at room temperature, we find that $\varepsilon \approx 2 \times 10^{-7}$.

To cast the equations in dimensionless form, we choose the Nusselt thickness, H, corresponding to a uniform steady isothermal flow given by

$$H = \left(\frac{3\mu_0 Q}{g \rho_0 \sin\beta}\right)^{1/3} ,$$

as the length scale, where Q denotes the constant volume flux. The pressure is scaled using $\rho_0 U^2$ with $U = Q/H$ being the velocity scale. The time scale is taken to be H/U and the scaled temperature difference is $T^* = (T - T_a)/\Delta T$, where $\Delta T = T_b - T_a$. Using the Boussinesq approximation, the dimensionless equations, with the asterisk removed from the scaled temperature for notational convenience, become

$$\frac{\partial u}{\partial x} + \frac{\partial w}{\partial z} = 0 , \tag{6}$$

$$Re \frac{Du}{Dt} = -Re \frac{\partial p}{\partial x} + 3(1 - \alpha T) + \frac{\partial}{\partial x}\left((1 - \lambda T)\frac{\partial u}{\partial x}\right) + \frac{\partial}{\partial z}\left((1 - \lambda T)\frac{\partial u}{\partial z}\right) - \lambda \frac{\partial T}{\partial x}\frac{\partial u}{\partial x} - \lambda \frac{\partial T}{\partial z}\frac{\partial w}{\partial x} , \tag{7}$$

$$Re \frac{Dw}{Dt} = -Re \frac{\partial p}{\partial z} - 3\cot\beta(1 - \alpha T) + \frac{\partial}{\partial x}\left((1 - \lambda T)\frac{\partial w}{\partial x}\right) + \frac{\partial}{\partial z}\left((1 - \lambda T)\frac{\partial w}{\partial z}\right) - \lambda \frac{\partial T}{\partial x}\frac{\partial u}{\partial z} - \lambda \frac{\partial T}{\partial z}\frac{\partial w}{\partial z} , \tag{8}$$

$$PrRe \frac{DT}{Dt} = \frac{\partial}{\partial x}\left[(1 + \Lambda T)\frac{\partial T}{\partial x}\right] + \frac{\partial}{\partial z}\left[(1 + \Lambda T)\frac{\partial T}{\partial z}\right] , \tag{9}$$

where the Reynolds number is $Re = \rho_0 U H/\mu_0$, the Prandtl number is $Pr = \mu_0 c_p/K_0$, and $\alpha = \hat{\alpha}\Delta T/\rho_0$, $\lambda = \hat{\lambda}\Delta T/\mu_0$, and $\Lambda = \hat{\Lambda}\Delta T/K_0$.

The dynamic conditions along the free surface, $z = h(x,t)$, are

$$p = \frac{2(1 - \lambda T)}{ReF}\left(\left[\frac{\partial h}{\partial x}\right]^2 \frac{\partial u}{\partial x} + \frac{\partial w}{\partial z} - \frac{\partial h}{\partial x}\frac{\partial u}{\partial z} - \frac{\partial h}{\partial x}\frac{\partial w}{\partial x}\right) - \frac{(We - MaT)}{F^{3/2}}\frac{\partial^2 h}{\partial x^2} \tag{10}$$

and

$$-MaRe\sqrt{F}\left(\frac{\partial T}{\partial x} + \frac{\partial h}{\partial x}\frac{\partial T}{\partial z}\right) = (1 - \lambda T)\left[G\left(\frac{\partial u}{\partial z} + \frac{\partial w}{\partial x}\right) - 4\frac{\partial h}{\partial x}\frac{\partial u}{\partial x}\right] , \tag{11}$$

where

$$F = 1 + \left[\frac{\partial h}{\partial x}\right]^2 , \; G = 1 - \left[\frac{\partial h}{\partial x}\right]^2 ,$$

$We = \sigma_0/(\rho_0 U^2 H)$ is the Weber number and $Ma = \gamma \Delta T/(\rho_0 U^2 H)$ is the Marangoni number.

Based on Newton's law of cooling, the heat transfer across the free surface in non-dimensional form can be expressed as

$$- Bi\sqrt{F}T = (1 + \Lambda T)\left(\frac{\partial T}{\partial z} - \frac{\partial h}{\partial x}\frac{\partial T}{\partial x}\right) , \tag{12}$$

where $Bi = \alpha_g H/K_0$ is the Biot number while α_g denotes the heat transfer coefficient across the liquid-air interface.

Ignoring the evaporation of fluid along the free surface, $z = h(x,t)$, leads to the following kinematic condition:

$$w = \frac{\partial h}{\partial t} + u\frac{\partial h}{\partial x} .$$

A no-slip condition is applied at the impermeable inclined planar surface which gives us

$$u = w = 0 \text{ at } z = 0 . \tag{13}$$

Finally, the constant bottom temperature condition is given by

$$T = 1 \text{ at } z = 0 . \tag{14}$$

III. STABILITY ANALYSIS

We begin by denoting the steady-state flow by $u = u_s(z)$, $w = w_s(z)$, $p = p_s(z)$, and $T = T_s(z)$. With the adopted scaling, the uniform film thickness is $h_s \equiv 1$ and it also follows that $w_s(z) \equiv 0$. We next proceed to determine exact expressions for $u_s(z)$, $p_s(z)$, and $T_s(z)$ and introduce the differential operator D where $D \equiv d/dz$.

The steady-state temperature, $T_s(z)$, satisfies

$$D[(1 + \Lambda T_s)DT_s] = 0 , \tag{15}$$

subject to the heat transfer condition along the interface

$$(1 + \Lambda T_s)DT_s + BiT_s = 0 \;\text{ at }\; z = 1 , \tag{16}$$

and the constant bottom temperature condition

$$T_s(0) = 1 . \tag{17}$$

The solution is given by

$$T_s(z) = \sqrt{a - bz} - \frac{1}{\Lambda} ,$$

where

$$a = \frac{(1+\Lambda)^2}{\Lambda^2} , \; b = \frac{2Bi(1+Bi)}{\Lambda^2}\left[\sqrt{1 + \frac{((1+\Lambda)^2 - 1)}{(1+Bi)^2}} - 1\right] .$$

It is worth noting that the above solution collapses to known solutions for special cases. For example, when $\Lambda = 0$, the above simplifies to

$$T_s(z) = 1 - \frac{Bi}{1+Bi}z .$$

Thus, when $Bi = 0$, we have $T_s(z) = 1$, while when $Bi \to \infty$, we obtain $T_s(z) = 1 - z$. The physical interpretations associated with these cases are as follows. For constant thermal conductivity (i.e., $\Lambda = 0$), the case when $Bi = 0$ corresponds to an insulated fluid layer having a uniform temperature equal to that of the bottom (T_b). On the other hand, as $Bi \to \infty$, this corresponds to an infinite rate of heat transfer across the interface

which means that the interface temperature will remain at the ambient temperature (T_a) resulting in a linear temperature profile.

The steady-state streamwise velocity, $u_s(z)$, satisfies

$$D[(1-\lambda T_s)Du_s] + 3(1-\alpha T_s) = 0 \tag{18}$$

and is subject to the stress-free condition along the interface

$$Du_s = 0 \ \text{ at } \ z = 1 \tag{19}$$

and the no-slip condition on the bottom

$$u_s(0) = 0\ . \tag{20}$$

The solution is given by

$$u_s(z) = a_0 \ln\left(\frac{A-\lambda\sqrt{a-bz}}{A-\lambda\sqrt{a}}\right) + a_1 z - \frac{\alpha}{\lambda}z^2 + a_2(\sqrt{a-bz}-\sqrt{a}) + a_3[(a-bz)^{3/2} - a^{3/2}]\ ,$$

where

$$a_0 = \frac{2AB}{b\lambda^2} + \frac{6AC(1+\frac{\alpha}{\Lambda})}{b^2\lambda^2} - \frac{4\alpha A^4}{b^2\lambda^5}\ ,\ a_1 = \frac{2\alpha}{b\lambda}(C+2a) - \frac{3A(1+\frac{\alpha}{\Lambda})}{b\lambda^2}\ ,\ a_2 = \frac{6C(1+\frac{\alpha}{\Lambda})}{b^2\lambda} + \frac{2B}{b\lambda} - \frac{4\alpha A^3}{b^2\lambda^4}\ ,$$
$$a_3 = \frac{2(1+\frac{\alpha}{\Lambda})}{b^2\lambda} - \frac{4\alpha A}{3b^2\lambda^2}\ ,\ A = 1+\frac{\lambda}{\Lambda}\ ,\ B = 3\left(1+\frac{\alpha}{\Lambda}\right) + \frac{2\alpha}{b}(a-b)^{3/2}\ ,\ C = \frac{A^2}{\lambda^2} - a\ .$$

For the special case, when $Bi = 0$, the above collapses to

$$u_s(z) = 3\left(\frac{1-\alpha}{1-\lambda}\right) z\left(1-\frac{z}{2}\right)\ ,$$

while when $Bi \to \infty$ together with $\Lambda = 0$, we obtain

$$u_s(z) = \frac{3}{4\lambda^3}\ \big[-\alpha\, z^2\lambda^2 - 4\, z\lambda^2 + 2\,\alpha\, z\lambda^2 + 2\,\alpha\, z\lambda + 4\,\ln(z\lambda+1-\lambda)\,\lambda$$
$$-2\,\ln(z\lambda+1-\lambda)\,\alpha - 4\,\ln(1-\lambda)\,\lambda + 2\,\ln(1-\lambda)\,\alpha\big]\ .$$

Another special case occurs when $\lambda = \Lambda = 0$; here, the above simplifies to

$$u_s(z) = -\frac{z}{2}\left[3(1-\alpha)z - 6 + \frac{\alpha Bi}{1+Bi}z^2 + \frac{3\alpha(2+Bi)}{1+Bi}\right].$$

Finally, in the isothermal limit we expect the above expression to recover the familiar parabolic profile given by $u_s(z) = 3z(1-z/2)$.

Finally, the steady-state pressure, $p_s(z)$, can be obtained by solving

$$ReDp_s = -3\cot\beta(1-\alpha T_s)\ , \tag{21}$$

subject to

$$p_s(1) = 0\ . \tag{22}$$

The solution is easily found to be

$$p_s(z) = \frac{3\cot\beta}{Re}\left(1+\frac{\alpha}{\Lambda}\right)(1-z) + \frac{2\alpha\cot\beta}{bRe}[(a-b)^{3/2} - (a-bz)^{3/2}]\ .$$

To investigate the stability of the steady-state flow, we perturb the flow by introducing infinitesimal disturbances and then monitor how the disturbances evolve in time. The perturbed flow is expressed as

$$u = u_s(z) + \tilde{u}(x,z,t)\ ,\ w = \tilde{w}(x,z,t)\ ,\ p = p_s(z) + \tilde{p}(x,z,t)\ ,\ T = T_s(z) + \tilde{T}(x,z,t)\ ,\ h = 1 + \tilde{\eta}(x,t)\ ,$$

where $\tilde{\eta}$ is the imposed perturbation in the fluid thickness while the tilde denotes perturbations in the other quantities. The perturbations are assumed to have the form

$$(\tilde{u},\tilde{w},\tilde{p},\tilde{T},\tilde{\eta}) = (\hat{u}(z),\hat{w}(z),\hat{p}(z),\hat{T}(z),\hat{\eta})e^{ik(x-ct)}\ ,$$

which represent waves propagating in the x direction with z-dependent amplitudes. Here, k denotes the wavenumber and is taken to be real and positive, while c is a complex quantity where the real part is the phase speed and the imaginary part, denoted by $\mathrm{Im}(c)$, is related to the growth rate.

Substituting the perturbed flow into the governing equations and linearizing leads to the following equations for the z-dependent amplitudes:

$$D\hat{w} + ik\hat{u} = 0 \,, \tag{23}$$

$$\begin{aligned} Re[ik(u_s - c)\hat{u} + \hat{w}Du_s] = -ikRe\hat{p} + k^2(\lambda T_s - 1)\hat{u} + \\ D[(1 - \lambda T_s)D\hat{u}] - \lambda\hat{T}D^2u_s - \lambda Du_s D\hat{T} - ik\lambda\hat{w}DT_s - 3\alpha\hat{T} \,, \end{aligned} \tag{24}$$

$$\begin{aligned} ikRe(u_s - c)\hat{w} = -ReD\hat{p} + 3\alpha\cot\beta\,\hat{T} - k^2(1 - \lambda T_s)\hat{w} + \\ D[(1 - \lambda T_s)D\hat{w}] - ik\lambda\hat{T}Du_s - \lambda DT_s D\hat{w} \,, \end{aligned} \tag{25}$$

$$PrRe[ik(u_s - c)\hat{T} + \hat{w}DT_s] = -k^2(1 + \Lambda T_s)\hat{T} + D^2[(1 + \Lambda T_s)\hat{T}] \,. \tag{26}$$

Expanding the boundary conditions at $z = 1 + \tilde{\eta}$ about $z = 1$ and linearizing yields the conditions

$$\hat{p} = -\hat{\eta}Dp_s + \frac{2}{Re}(1 - \lambda T_s)D\hat{w} + k^2(We - MaT_s)\hat{\eta} \,, \tag{27}$$

$$(1 - \lambda T_s)(\hat{\eta}D^2u_s + D\hat{u} + ik\hat{w}) = -ikMaRe(\hat{T} + \hat{\eta}DT_s) \,, \tag{28}$$

$$D[(1 + \Lambda T_s)\hat{T}] + \hat{\eta}D[(1 + \Lambda T_s)DT_s + BiT_s] + Bi\hat{T} = 0 \,, \tag{29}$$

$$\hat{w} = ik(u_s - c)\hat{\eta} \tag{30}$$

at $z = 1$. At $z = 0$, we have

$$\hat{u}(0) = \hat{w}(0) = \hat{T}(0) = 0 \,. \tag{31}$$

The system of equations (23)-(31) is posed as an eigenvalue problem with c denoting the eigenvalue. We next take advantage of the fact that small wavenumber perturbations are expected to be most unstable, and consequently an asymptotic analysis as $k \to 0$ predicts the onset of instability. While this is obviously true for the isothermal case, numerical solutions for the non-isothermal case with constant fluid properties also reveal that small wavenumber perturbations are the most unstable.[13] Based on this, we proceed by expanding the perturbations in powers of k as follows:

$$\begin{aligned} \hat{u} &= \hat{u}_0(z) + k\hat{u}_1(z) + O(k^2) \,, \\ \hat{w} &= \hat{w}_0(z) + k\hat{w}_1(z) + O(k^2) \,, \\ \hat{p} &= \hat{p}_0(z) + k\hat{p}_1(z) + O(k^2) \,, \\ \hat{T} &= \hat{T}_0(z) + k\hat{T}_1(z) + O(k^2) \,, \\ \hat{\eta} &= \hat{\eta}_0 + k\hat{\eta}_1 + O(k^2) \,. \end{aligned}$$

The eigenvalue is similarly expanded as

$$c = c_0 + kc_1 + O(k^2)$$

with the understanding that the growth rate is given by $k\mathrm{Im}(c)$, and neutral stability occurs when $\mathrm{Im}(c) = 0$. Without loss of generality, we normalize the eigenvalue problem by setting $\hat{\eta}_0 = 1$ and $\hat{\eta}_1 = 0$.[14] When the above are substituted into (23)-(31), we obtain a hierarchy of problems at various orders of k.

The leading-order problem satisfies

$$D\hat{w}_0 = 0 \,, \tag{32}$$

$$D^2[(1 + \Lambda T_s)\hat{T}_0] = 0 \,, \tag{33}$$

$$ReD\hat{p}_0 = 3\alpha\cot\beta\hat{T}_0 \,, \tag{34}$$

$$D[(1 - \lambda T_s)D\hat{u}_0] = 3\alpha\hat{T}_0 + \lambda D(\hat{T}_0 Du_s) \,, \tag{35}$$

subject to

$$\hat{w}_0(0) = 0 \,, \tag{36}$$

$$D[(1 + \Lambda T_s)\hat{T}_0] + BiDT_s = -Bi\hat{T}_0 \ \text{ at } \ z = 1 \,, \ \hat{T}_0(0) = 0 \,, \tag{37}$$

$$\hat{p}_0 = -Dp_s \ \text{ at } \ z = 1, \tag{38}$$

$$D\hat{u}_0 = -D^2u_s \ \text{ at } \ z = 1 \,, \ \hat{u}_0(0) = 0 \,. \tag{39}$$

The system (32)-(34) has the solution

$$\hat{w}_0(z) = 0\,,$$
$$\hat{T}_0(z) = \frac{e_0 z}{\sqrt{a-bz}}\,,$$
$$\hat{p}_0(z) = e_1 - \frac{6\alpha e_0 \cot\beta}{bRe} z\sqrt{a-bz} - \frac{4\alpha e_0 \cot\beta}{b^2 Re}(a-bz)^{3/2}\,,$$

where

$$e_0 = \frac{Bi^2\left[\sqrt{(1+Bi)^2+(1+\Lambda)^2-1}-(1+Bi)\right]}{\Lambda^2\sqrt{(1+Bi)^2+(1+\Lambda)^2-1}}\,,$$
$$e_1 = \frac{3\cot\beta}{Re}\left(1+\frac{\alpha}{\Lambda}\right) - \frac{3\alpha\cot\beta}{Re}\left(1-\frac{2e_0}{b}\right)\sqrt{a-b} + \frac{4\alpha e_0\cot\beta}{b^2 Re}(a-b)^{3/2}\,.$$

The solution to (35) has the form

$$\hat{u}_0(z) = b_0 + b_1 z + b_2(a-bz)^{3/2} + b_3\ln(a-bz) + b_4\sqrt{a-bz} + \frac{b_5}{A-\lambda\sqrt{a-bz}} + b_6\ln(A-\lambda\sqrt{a-bz})\,,$$

where the constants b_j $(j = 0,1,\ldots,6)$ are lengthy expressions involving many of the previously defined constants.

At $O(k)$, the problem becomes

$$Dw_1 = -\hat{u}_0\,, \tag{40}$$
$$D^2[(1+\Lambda T_s)T_1] = PrRe[(u_s - c_0)\hat{T}_0 + w_1 DT_s]\,, \tag{41}$$
$$D[(1-\lambda T_s)Du_1] = 3\alpha T_1 + \lambda D(T_1 Du_s) + Re[\hat{p}_0 + (u_s - c_0)\hat{u}_0 + w_1 Du_s]\,, \tag{42}$$

subject to

$$w_1(0) = 0\,, \tag{43}$$
$$D[(1+\Lambda T_s)T_1] = -BiT_1 \ \text{ at } \ z = 1\,,\ T_1(0) = 0\,, \tag{44}$$
$$(1-\lambda T_s)Du_1 = -MaRe(\hat{T}_0 + DT_s) \ \text{ at } \ z = 1\,,\ u_1(0) = 0\,, \tag{45}$$

where $\hat{w}_1(z) = iw_1(z)$, $\hat{T}_1(z) = iT_1(z)$, and $\hat{u}_1(z) = iu_1(z)$ are complex-valued functions while $w_1(z)$, $T_1(z)$, and $u_1(z)$ are real-valued functions. The solution to (40) has the form

$$w_1(z) = d_0 + d_1 z + d_2 z^2 + d_3(a-bz)^{3/2} + d_4(a-bz)^{5/2} + d_5 z\ln(a-bz)$$
$$+ d_6\ln(a-bz) + d_7\sqrt{a-bz} + d_8(a-bz)\ln(A-\lambda\sqrt{a-bz}) + d_9\ln(A-\lambda\sqrt{a-bz})\,,$$

where the constants d_l $(l = 0,1,\ldots,9)$ are related to b_j $(j = 0,1,\ldots,6)$. Solutions to (41) and (42) were obtained with the help of the Maple Computer Algebra System but are very lengthy and hence not worth presenting explicitly; instead, we include the Maple code.[15] The expression for u_1 involves the dilogarithm (dilog(z)) and the general polylogarithm of index m (polylog(m,z)) functions defined by

$$\text{dilog}(z) = \int_1^z \frac{\ln(\xi)}{(1-\xi)}d\xi\ ,\ \ \text{polylog}(m,z) = \sum_{n=1}^{\infty}\frac{z^n}{n^m}\ .$$

We point out that the phase speed corresponding to the most unstable disturbance occurs when $k = 0$ (i.e., infinitely long wavelength) and hence is given by c_0. From the kinematic condition, it follows that:

$$c_0 = u_s(1) - w_1(1) \tag{46}$$

and is a real quantity. To obtain the condition for neutral stability, we proceed to the $O(k^2)$ problem and examine the equation

$$D\hat{w}_2 = -i\hat{u}_1 \tag{47}$$

and the corresponding impermeability condition

$$\hat{w}_2(0) = 0\,. \tag{48}$$

Since $\hat{u}_1(z)$ is imaginary, it follows that $\hat{w}_2(z)$ will be a real-valued function. Applying the kinematic condition yields

$$c_1 = i\hat{w}_2(1)\,.$$

Thus, the condition $\mathrm{Im}(c) = 0$ for neutral stability reduces to $c_1 = 0$ or

$$\int_0^1 u_1(\xi)d\xi = 0 \ . \tag{49}$$

Solving (49) generates a dispersion relation for the scaled critical Reynolds number, $Re^*_{crit} = Re_{crit}/\cot\beta$, having the functional form

$$Re^*_{crit} = f(\alpha, \lambda, \Lambda, Pr, Ma, Bi) \ ,$$

which predicts the onset of instability. Turning off the heating recovers the familiar isothermal result $Re^*_{crit} = 5/6$. Also, just as in the isothermal case, for Weber numbers of order unity, the critical Reynolds number does not depend on We. Apart from the two special cases corresponding to $Bi = 0$ and $\lambda = \Lambda = 0$ outlined in Ref. 10, the analytical expression for Re^*_{crit} is extremely lengthy and complicated. Fortunately, with the help of the Maple Computer Algebra System, we are able to produce plots illustrating how the scaled critical Reynolds number, Re^*_{crit}, and perturbation phase speed, c_0, depend on the various dimensionless parameters. This is the focus of Sec. IV.

IV. RESULTS AND DISCUSSION

Based on the dimensionless formulae

$$\frac{\rho}{\rho_0} = 1 - \alpha T \ , \quad \frac{\mu}{\mu_0} = 1 - \lambda T \ ,$$

and the fact that the scaled temperature, T, attains a maximum value of unity, it immediately follows that $\alpha, \lambda \in [0, 1)$.

We begin by making comparisons with previous research. Pascal *et al.*[10] derived asymptotic expansions for Re^*_{crit} for cases when $Bi \to 0$ and when $\lambda, \Lambda \to 0$. Contrasted in Figure 1 are exact and asymptotic variations in Re^*_{crit} with Bi. Two different asymptotic expansions are captured in this plot, one for small Bi and the other for small λ, Λ. As expected good agreement is found in the small Bi limit. Since the values of λ, Λ are fairly small, we also see good agreement over the entire range of Bi shown. The extent of validity of the asymptotic expansions is clearly demonstrated in Figure 2. Again, two different asymptotic expansions are illustrated here. The asymptotic expansion for small Bi agrees well with the exact solution provided Bi is small, while the other shows poor agreement since the values of λ, Λ are larger in this case.

In interpreting our results, we first consider the case with $Bi = 0$. This corresponds to the idealized case where no heat escapes through the surface of the fluid layer, and consequently the steady temperature distribution is uniform. In this case, the scaled critical Reynolds number reduces to

$$Re^*_{crit} = \frac{5}{6}\frac{(1-\lambda)^2}{(1-\alpha)} \ .$$

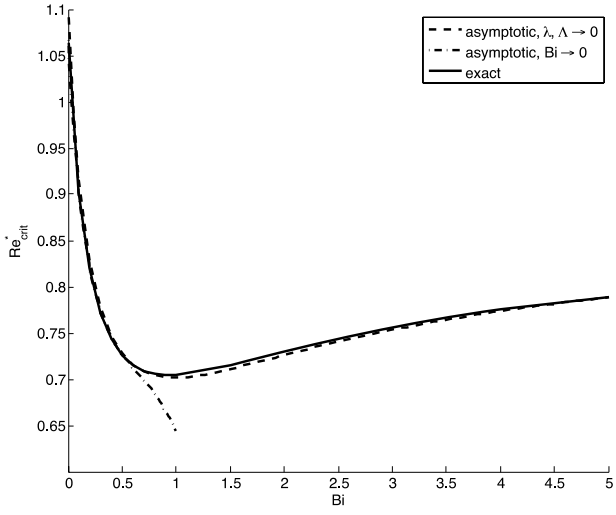

FIG. 1. Comparison between exact and asymptotic Re^*_{crit} values with $\alpha = 0.5$, $\lambda = 0.2$, $\Lambda = 0.25$, $Ma = 1$, and $Pr = 7$.

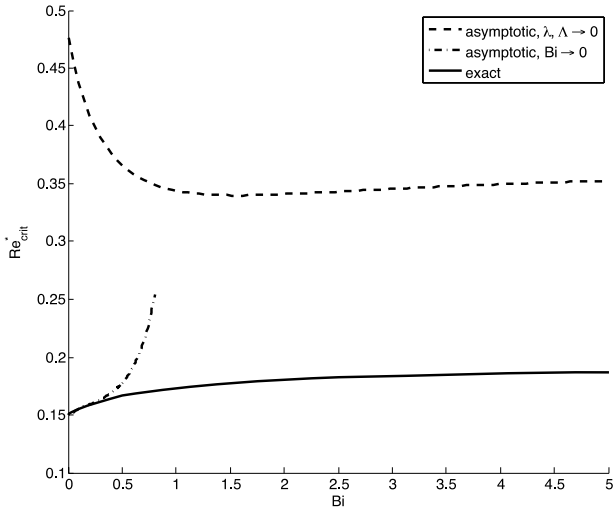

FIG. 2. Comparison between exact and asymptotic Re^*_{crit} values with $\alpha = 0.5$, $\lambda = 0.7$, $\Lambda = 0.7$, $Ma = 1$, and $Pr = 7$.

Thus, Re^*_{crit} increases with α and decreases with λ. This can be explained by examining how the flow rate, Q, is influenced. Recall that for a steady uniform isothermal flow,

$$Q = \frac{\rho g \sin\beta H^3}{3\mu} .$$

We immediately see that increasing α decreases ρ, and hence, decreases the flow rate which stabilizes the flow when μ is kept constant. Likewise, if we fix ρ and increase λ, then μ decreases which increases the flow rate, and thus destabilizes the flow. Alternatively, increasing λ reduces the viscosity and gives rise to a less viscous fluid which will result in a greater flow rate. It is interesting to note that if λ varies according to $\lambda = 1 - \sqrt{1-\alpha}$, then Re^*_{crit} remains constant.

If we now let Bi increase from zero the temperature distribution in the fluid begins to develop a negative z gradient and if the free surface is non-planar, then the temperature along the free surface will no longer be constant. One important consequence will of course be the generation of thermocapillarity. We can isolate this effect by setting $\lambda = \Lambda = \alpha = 0$, i.e., allowing surface tension to be the only fluid property that varies with temperature. In this case, the expression for the scaled critical Reynolds number is given by

$$Re^*_{crit} = \frac{10(1+Bi)^2}{5Ma\,Bi + 12(1+Bi)^2} ,$$

which coincides with the result obtained in previous research.[5] This formula clearly shows that thermocapillarity is destabilizing since Re^*_{crit} decreases with Ma. As a function of Bi, the scaled critical Reynolds number attains a minimum at $Bi = 1$, given by $Re^*_{crit,min} = 40/(48 + 5Ma)$, and the limit as Bi tends to infinity is equal to the value at $Bi = 0$ which is given by $Re^*_{crit} = 5/6$; this corresponds to the well known theoretical result for the isothermal case. This dependence on Bi can be explained as follows. When $Bi = 0$, the steady-state temperature within the fluid layer is constant, and thus the free-surface temperature is uniform which neutralizes the Marangoni effect. As Bi is increased, a variation in free-surface temperature develops and thermocapillary forces are strengthened. However, for large Bi, the temperature along the free surface approaches that of the ambient medium which is constant, and as such the Marangoni effect is again weakened. Consequently, there exists a optimal value of Bi for which thermocapillarity is maximized resulting in a minimum value for Re^*_{crit}.

We next examine the impact of variation in the density with respect to z, which occurs when the Biot number is in the range of $0 < Bi < \infty$. For positive and finite Bi, a negative temperature gradient within the fluid layer ensues which establishes a gravitationally unstable top-heavy density gradient within the fluid layer. We expect an amplification in the temperature gradient to be a contributor to flow instability since it affects the density gradient (i.e., $\partial/\partial z(\rho/\rho_0) = -\alpha\partial T/\partial z$). Furthermore, changes in surface elevation will cause changes in the flow rate which will accentuate surface undulations and lead to instability. Finally, the variation in free-surface temperature is maximized at an optimal value of Bi which maximizes the variation in density along an undulating surface which in turn plays a destabilizing role similar to a variable surface tension. The physical interpretation is that a variable free-surface density will lead to variations in momentum which will

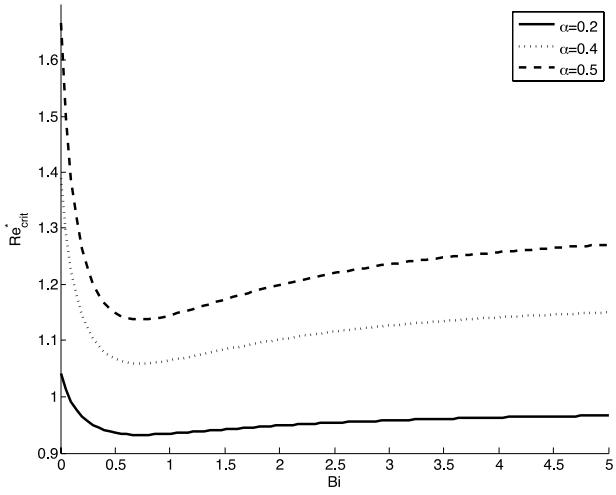

FIG. 3. Re^*_{crit} versus Bi for selected values of α with $\lambda = \Lambda = Ma = 0$, and $Pr = 7$.

generate impulses and create surges. Now, increasing the parameter α amplifies the density gradient and thus magnifies the instability mechanisms listed above. However, the density decreases as α is increased and this will lower the flow rate. Thus, increasing α triggers competing stability mechanisms. This competition is also reflected in the Rayleigh number, Ra, which for our formulation and flow configuration can be expressed as

$$Ra = \frac{\hat{\alpha} g \cos\beta H^3 \Delta T}{\rho_0 \left(\frac{\mu}{\rho}\right)\left(\frac{K}{\rho c_p}\right)} = 3\cot\beta\left(\frac{\alpha c_p \rho^2 Q}{\rho_0 K}\right).$$

In the classical Rayleigh-Bénard problem,[16,17] the Rayleigh number represents the ratio of the destabilizing effect of the buoyancy force to the stabilizing effect of the viscous force. Here, we clearly see that increasing α does not necessarily increase Ra since both ρ and Q decrease while holding c_p and K constant. The outcome of this interaction will be further influenced by the other parameters, which we now investigate.

We begin by setting all the temperature variation parameters equal to zero except α, i.e., $\lambda = \Lambda = Ma = 0$. In this case, the scaled critical Reynolds number will only depend on α, Bi, and Pr. The dependence on these parameters is illustrated in Figures 3 and 4. Figure 3 shows Re^*_{crit} as a function of Bi for different values of α with $Pr = 7$, while in Figure 4, the Prandtl number is fixed at a value of 30. It can be seen that in all cases,

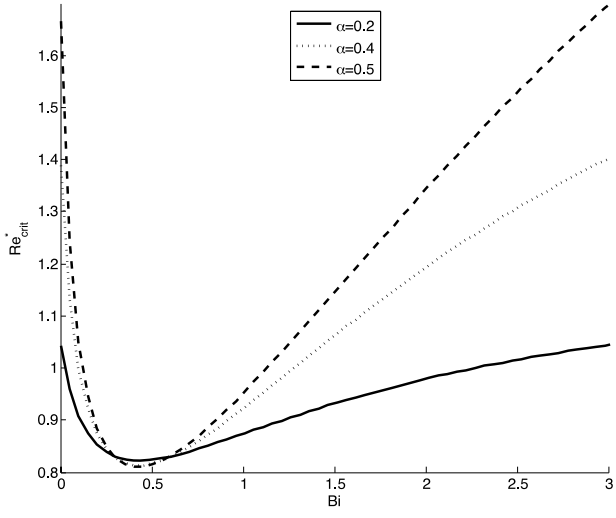

FIG. 4. Re^*_{crit} versus Bi for selected values of α with $\lambda = \Lambda = Ma = 0$, and $Pr = 30$.

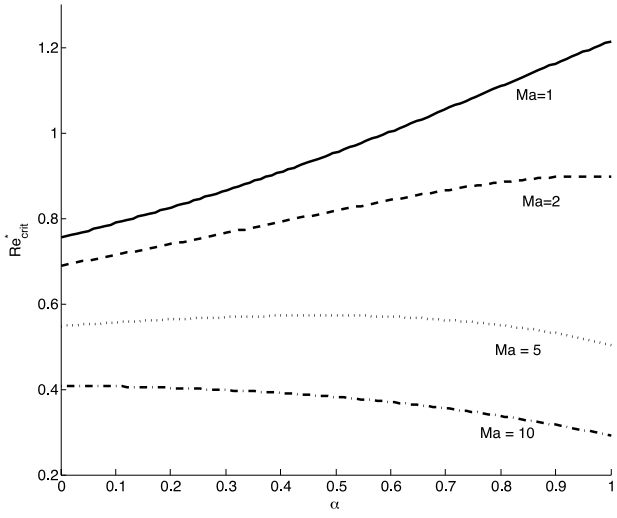

FIG. 5. Re^*_{crit} versus α for selected values of Ma with $\lambda = \Lambda = 0$, $Bi = 1$, and $Pr = 7$.

Re^*_{crit} attains a minimum at an intermediate value of Bi. This behaviour is similar to that associated with thermocapillarity as explained above and is related to variations in density along the surface as well as variations in flow rate. An interesting difference, however, is the fact that as Bi tends to infinity, Re^*_{crit} does not approach the value corresponding to $Bi = 0$. Instead, it approaches a value that varies with α and Pr according to the formula

$$Re^*_{crit} = \frac{1008(40 - 11\,\alpha)}{48384 + 7285\,\alpha^2 - 1575\,\alpha\,Pr + 465\,\alpha^2 Pr - 37863\,\alpha}\ .$$

It can be shown that for $Pr < Pr_c$, the limit is less than the value at $Bi = 0$ which is $Re^*_{crit} = \frac{5}{6(1-\alpha)}$, while for $Pr > Pr_c$, the opposite is true. The value of Pr_c is given by

$$Pr_c = \frac{119133 - 30103\,\alpha}{75(105 - 31\,\alpha)}\ .$$

For $0 < \alpha < 1$, the value of Pr_c ranges between $1891/125 \approx 15$ and $8903/555 \approx 16$.

Regarding the outcome of increasing α, the results in Figure 3 reveal that for fixed values of Bi and Pr, the scaled critical Reynolds number increases. The rise in Re^*_{crit} is particularly dramatic for small values of Bi since in this range, the stratification is weak and the free-surface temperature is nearly uniform; thus all

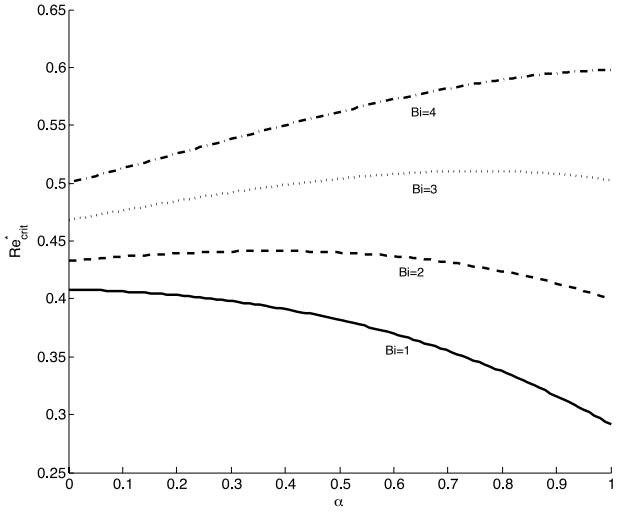

FIG. 6. Re^*_{crit} versus α for selected values of Bi with $\lambda = \Lambda = 0$, $Ma = 10$, and $Pr = 7$.

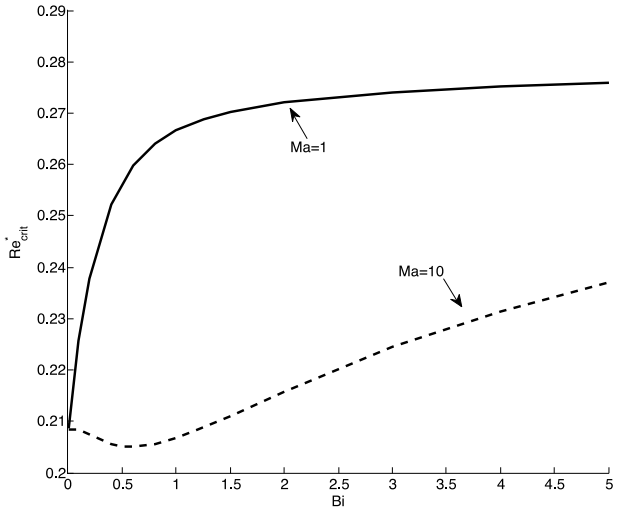

FIG. 7. Re^*_{crit} as a function of Bi for selected values of Ma with $\lambda = 0.5$, $\alpha = \Lambda = 0$, and $Pr = 7$.

the destabilizing factors are minimized. However, as it can be seen in Figure 4, if Pr is sufficiently large then increasing α can destabilize the flow for a specific range of Bi values.

Now, we proceed to study the interaction with the Marangoni effect. Figure 5 portrays plots of Re^*_{crit} as a function of α for different values of Ma with $Bi = 1$ and $Pr = 7$. It can be seen that if Ma is sufficiently large, increasing α destabilizes the flow. This suggests that the Marangoni effect couples with the destabilizing effects associated with a variable density, and if sufficient, it can reverse the outcome of the competition between stabilizing and destabilizing factors.

In Figure 6, we display Re^*_{crit} as a function of α for various values of Bi with $Ma = 10$. For sufficiently large Bi, the free-surface temperature has little variation, and thermocapillarity is weak despite the large Marangoni number. Therefore, increasing α acts as a stabilizing factor as in the case for small Ma. As Bi is decreased and approaches the optimal value for which the Marangoni effect is maximized, the stabilizing influence of α diminishes and eventually succumbs to thermocapillarity.

Varying λ in conjunction with other parameters has a more complicated outcome. Figure 7 plots variations in Re^*_{crit} with Bi for selected values of Ma with $\lambda = 0.5$. In contrast to the case with $\lambda = 0$ illustrated in Figures 3 and 4, it is evident that if λ is sufficiently large and Ma sufficiently small, then Re^*_{crit} becomes an increasing function of Bi. This phenomenon is explained as follows. If $Bi = 0$, then $T_s(z) \equiv 1$ and the

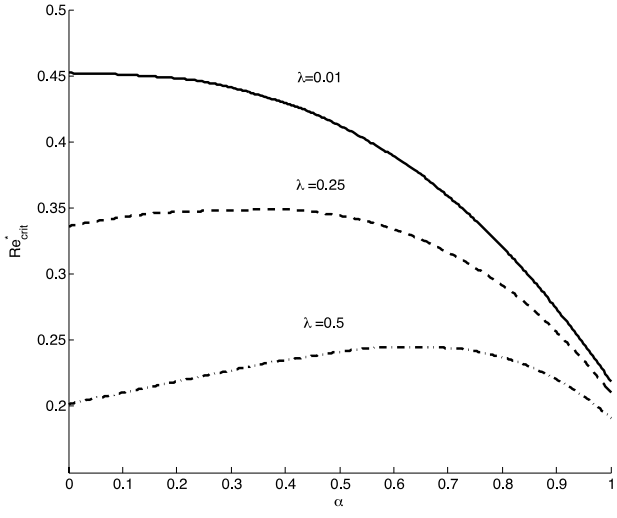

FIG. 8. Re^*_{crit} as a function of α for different λ with $Bi = 0.5$, $\Lambda = 0.5$, $Ma = 10$, and $Pr = 7$.

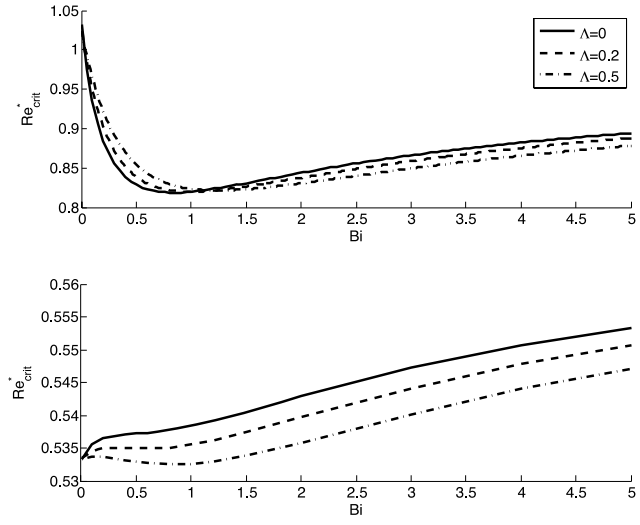

FIG. 9. Re^*_{crit} as a function of Bi for different values of Λ with $Ma = 1$ and $Pr = 7$. In the top panel, $\alpha = 0.2$ and $\lambda = 0$, while in the bottom panel, $\alpha = 0$ and $\lambda = 0.2$.

viscosity is reduced by the maximum amount throughout the fluid layer yielding a maximum flow rate. As Bi increases, T_s becomes a decreasing function of z, and thus the reduction in viscosity is less which leads to a decrease in flow rate and hence an increase in Re^*_{crit}. Although the Marangoni effect is strengthened as Bi increases from zero, for sufficiently small Ma, it is not enough to counterbalance the stabilizing effect associated with the increase in viscosity. For larger Ma, the variation in Re^*_{crit} with Bi possesses a minimum. As previously explained, the reason for this minimum is because there exists an optimal value of Bi where the Marangoni effect is maximized. In addition, the variation in viscosity along a non-planar surface will lead to changes in flow speed which will cause wave steepening that reinforces the Marangoni effect. Thus, these two effects combine to yield a significant decrease in Re^*_{crit} as seen in Figure 7.

Plotted in Figure 8 is Re^*_{crit} as a function of α for different values of λ. These results reveal that for small values of λ, the scaled critical Reynolds number is a decreasing function of α, whereas for larger λ, the distribution attains a maximum at an α value which increases with λ. As expected, for a fixed value of α, increasing λ destabilizes the flow since the fluid becomes less viscous. However, for a fixed value of λ increasing α can actually stabilize the flow if λ is sufficiently large. Again, we have competing effects which, depending on the parameter values, will dominate one over the other.

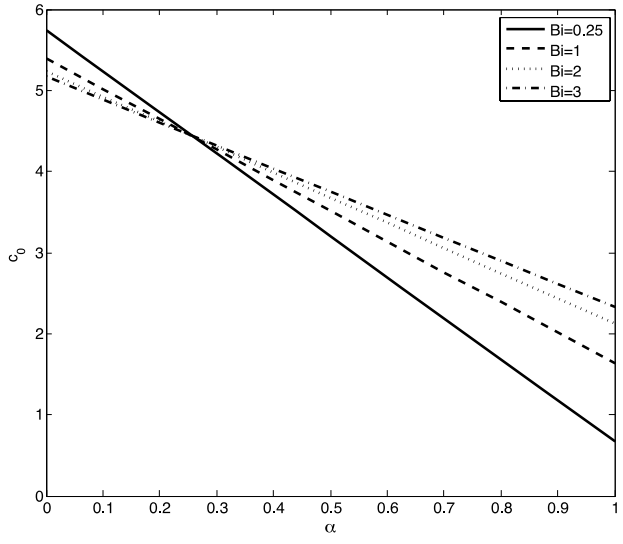

FIG. 10. c_0 versus α for selected values of Bi with $\lambda = 0.5$ and $\Lambda = 0.5$.

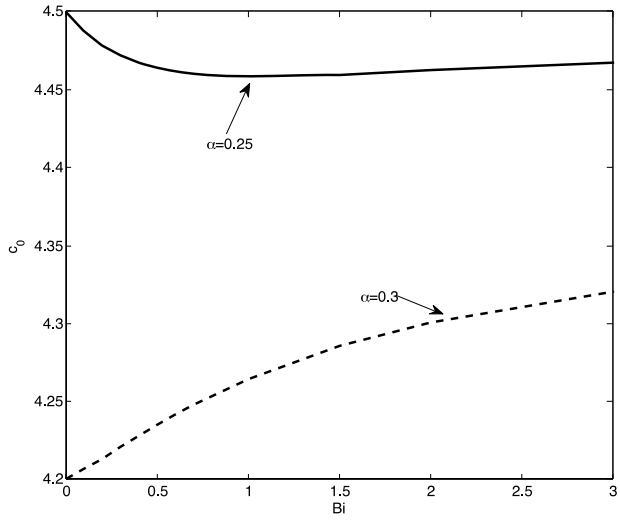

FIG. 11. c_0 versus Bi for selected values of α with $\lambda = 0.5$ and $\Lambda = 0.7$.

The rate of change in thermal conductivity with temperature is measured by Λ. As illustrated in Figure 9, the effect of this parameter on the onset of instability is dependent on the values of the other parameters. When plotted as a function of Bi, the results reveal that depending on the values of α and λ, the role played by increasing Λ can be reversed.

The last two figures attempt to reveal the dependence of the phase speed, c_0, on the various parameters. Analysing our expression for c_0, we have determined that it is independent of Ma and Pr. Furthermore, c_0 varies linearly with α; this feature is portrayed in Figure 10 for various values of Bi. Figures 10 and 11 indicate that the phase speed deviates significantly from the isothermal value $c_0 = 3$. Figure 11 which shows c_0 as a function of Bi, $c_0(Bi)$, for different values of α is particularly interesting; it illustrates that as α is increased, $c_0(Bi)$ changes from a function possessing a minimum to one that is strictly increasing.

V. CONCLUSIONS

Presented here was a theoretical investigation into the effects of variable fluid properties on thin film stability. The fluid properties were allowed to vary linearly with temperature. Heating takes place as a result of a temperature difference between the incline and the ambient gas. We carried out a linear stability analysis based on the assumption that long-wave perturbations are the most unstable. With the aid of the Maple Computer Algebra System, we were able to obtain exact solutions and compute the dependence of the critical Reynolds number and perturbation phase speed on the various dimensionless parameters controlling the problem. Previously, only asymptotic solutions to this problem were obtained that were restricted to small values of certain parameters. The present study is not subject to any of these restrictions; we were able to analyse the problem for the full range of parameter values and thus performed a more thorough investigation and drew new quantitative and qualitative conclusions.

More specifically, we studied in detail the effect of the density variation. Increasing α intensifies two competing effects regarding the onset of instability. One is a decrease in density throughout the fluid, which has a stabilizing effect since it reduces the flow rate. The other is related to the fact that the rate of reduction in density is height dependent resulting in a top-heavy stratification. This leads to a wave-breaking tendency which couples with thermocapillarity to amplify surface waviness and thus contributes to interfacial instability. We have illustrated how various other parameters affect the competition between these two effects. Most notably, we have discovered that if the increase in viscosity with height (due to a decrease in temperature) is sufficiently rapid, then the increase in flow rate with height is reduced allowing a decrease in density to stabilize the flow.

Another interesting observation that we discovered regards the coupling of variations in viscosity with the Marangoni effect. We found that if the viscosity variation is sufficiently large and Ma is sufficiently small, then the scaled critical Reynolds number becomes a strictly increasing function of Bi. However, for large enough values of Ma, the dependence of the scaled critical Reynolds number with Bi takes on a very different behaviour whereby the Re^*_{crit} curve possesses a minimum.

Finally, the formula obtained for the perturbation phase speed reveals that it is independent of Ma, Pr, and varies linearly with α.

[1] P. L. Kapitza and S. P. Kapitza, "Wave flow of thin layers of viscous fluid: III. Experimental study of undulatory flow conditions," Zh. Eksp. Teor. Fiz. **19**, 105-120 (1949), English translation in Collected Papers of P. L. Kapitza, edited by D. ter Haar (Pergamon, Oxford, 1965), Vol. II, pp. 690–709.
[2] T. B. Benjamin, "Wave formation in laminar flow down an inclined plane," J. Fluid Mech. **2**, 554-574 (1957).
[3] C.-S. Yih, "Stability of liquid flow down an inclined plane," Phys. Fluids **6**, 321-334 (1963).
[4] P. M. J. Trevelyan, B. Scheid, C. Ruyer-Quil, and S. Kalliadasis, "Heated falling films," J. Fluid Mech. **592**, 295-334 (2007).
[5] S. J. D. D'Alessio, J. P. Pascal, H. A. Jasmine, and K. A. Ogden, "Film flow over heated wavy inclined surfaces," J. Fluid Mech. **665**, 418-456 (2010).
[6] K. A. Ogden, S. J. D. D'Alessio, and J. P. Pascal, "Gravity-driven flow over heated, porous, wavy surfaces," Phys. Fluids **23**, 122102 (2011).
[7] D. A. Goussis and R. E. Kelly, "Effects of viscosity on the stability of film flow down heated or cooled inclined surfaces: Long-wavelength analysis," Phys. Fluids **28**, 3207-3214 (1985).
[8] C.-C. Hwang and C.-I. Weng, "Non-linear stability analysis of film flow down a heated or cooled inclined plane with viscosity variation," Int. J. Heat Mass Transfer **31**, 1775-1784 (1988).
[9] Y. O. Kabova and V. V. Kuznetsov, "Downward flow of a nonisothermal thin liquid film with variable viscosity," J. Appl. Mech. Tech. Phys. **43**, 895-901 (2002).
[10] J. P. Pascal, N. Gonputh, and S. J. D. D'Alessio, "Long-wave instability of flow with temperature dependent fluid properties down a heated incline," Int. J. Eng. Sci. **70**, 73-90 (2013).
[11] J. H. Spurk and N. Aksel, *Fluid Mechanics*, 2nd ed. (Springer, Berlin, Germany, 2008).
[12] D. J. Tritton, *Physical Fluid Dynamics* (Van Nostrand Reinhold, Cambridge, UK, 1977).
[13] S. Kalliadasis, C. Ruyer-Quil, B. Scheid, and M. G. Velarde, *Falling Liquid Films* (Springer-Verlag, London, UK, 2012).
[14] M. K. Smith, "The mechanism for the long-wave instability in thin liquid films," J. Fluid Mech. **217**, 469-485 (1990).
[15] See supplementary material at http://dx.doi.org/10.1063/1.4904095 for the symbolic algebra (Maple) code used to obtain the critical Reynolds number and the phase speed for the onset of instability.
[16] H. Bénard, "Les tourbillons cellulaires dans une nappe liquide," Rev. Gen. Sci. Pures Appl. **11**, 1261-1271 and 1309–1328 (1900).
[17] P. G. Drazin and W. H. Reid, *Hydrodynamic Stability*, 2nd ed. (Cambridge University Press, Cambridge, UK, 2004).